Am. J. Hum. Genet. 72:918–930, 2003

Refinement of a 400-kb Critical Region Allows Genotypic Differentiation between Isolated Lissencephaly, Miller-Dieker Syndrome, and Other Phenotypes Secondary to Deletions of 17p13.3

Carlos Cardoso,[1,2] Richard J. Leventer,[1,3] Heather L. Ward,[1] Kazuhito Toyo-oka,[4] June Chung,[1] Alyssa Gross,[1] Christa L. Martin,[1] Judith Allanson,[5] Daniela T. Pilz,[6] Ann H. Olney,[7] Osvaldo M. Mutchinick,[8] Shinji Hirotsune,[9] Anthony Wynshaw-Boris,[4] William B. Dobyns,[1] and David H. Ledbetter[1]

[1]Department of Human Genetics, University of Chicago, Chicago; [2]INSERM U491, Faculté de Médecine La Timone, Marseille; [3]Department of Neurology and Murdoch Children's Research Institute, Royal Children's Hospital, Melbourne; [4]Departments of Pediatrics and Medicine, University of California–San Diego School of Medicine, La Jolla, CA; [5]Division of Genetics, Children's Hospital of Eastern Ontario and University of Ottawa, Ottawa; [6]Institute for Medical Genetics, University Hospital of Wales, Cardiff; [7]Center for Human Genetics, University of Nebraska Medical Center, Omaha; [8]Departamento de Genética, Instituto Nacional de Ciencias Médicas y Nutrición Salvador Zubirán, Tlalpan, Mexico; and [9]Research Institute for Genomic Medicine, Saitama Medical School, Hidaka City, Japan

Deletions of 17p13.3, including the *LIS1* gene, result in the brain malformation lissencephaly, which is characterized by reduced gyration and cortical thickening; however, the phenotype can vary from isolated lissencephaly sequence (ILS) to Miller-Dieker syndrome (MDS). At the clinical level, these two phenotypes can be differentiated by the presence of significant dysmorphic facial features and a more severe grade of lissencephaly in MDS. Previous work has suggested that children with MDS have a larger deletion than those with ILS, but the precise boundaries of the MDS critical region and causative genes other than *LIS1* have never been fully determined. We have completed a physical and transcriptional map of the 17p13.3 region from *LIS1* to the telomere. Using fluorescence in situ hybridization, we have mapped the deletion size in 19 children with ILS, 11 children with MDS, and 4 children with 17p13.3 deletions not involving *LIS1*. We show that the critical region that differentiates ILS from MDS at the molecular level can be reduced to 400 kb. Using somatic cell hybrids from selected patients, we have identified eight genes that are consistently deleted in patients classified as having MDS. In addition, deletion of the genes *CRK* and *14-3-3ε* delineates patients with the most severe lissencephaly grade. On the basis of recent functional data and the creation of a mouse model suggesting a role for *14-3-3ε* in cortical development, we suggest that deletion of one or both of these genes in combination with deletion of *LIS1* may contribute to the more severe form of lissencephaly seen only in patients with MDS.

Introduction

Classical lissencephaly (LIS) is a severe brain malformation characterized by absent or reduced gyration of the cerebral surface and a thickened and simplified four-layered cortex resulting from incomplete neuronal migration during early brain development. Patients with LIS usually have mental retardation, intractable epilepsy, spasticity, and reduced longevity (Dobyns et al. 1993). The clinical severity generally correlates with the degree of agyria and cortical thickening. The complete LIS spectrum includes agyria (LIS grade 1), mixed agyria-pachygyria (LIS grades 2 and 3), and pachygyria alone (LIS grade 4) (Dobyns et al. 1999). The genetic basis of LIS has now been elucidated for most patients, with two main patterns evident. LIS more severe posteriorly than anteriorly is generally secondary to abnormalities of the *LIS1* gene (*PAFAH1B1* [MIM 601545]) on 17p13.3. This form of LIS is seen in both isolated lissencephaly sequence (ILS) and Miller-Dieker syndrome (MDS [MIM 247200]). LIS more severe anteriorly than posteriorly is generally due to abnormalities of the *DCX* gene (or *doublecortin* [MIM 300121]) on Xq22.3–q23 (Pilz et al. 1998*a*).

ILS is characterized by LIS and minimal or no other dysmorphic features. MDS is associated with LIS, significant facial dysmorphism, and, occasionally, other congenital anomalies, such as renal, gastrointestinal, and cardiac defects (table 1). In addition, the severity of LIS seen in MDS is generally greater than that seen in ILS (Dobyns et al. 1991). MDS is seen only in patients with deletions of 17p13.3, detected either by high-resolution cytogenetics or by the use of specific FISH

Received October 21, 2002; accepted for publication January 9, 2003; electronically published March 5, 2003.

Address for correspondence and reprints: David H. Ledbetter, Ph.D., Department of Human Genetics, The University of Chicago, 920 East 58th Street, Chicago, IL 60637. E-mail: dhl@genetics.uchicago.edu

0002-9297/2003/7204-0013$15.00

Table 1

Clinical Manifestations Observed in Patients with ILS versus Patients with MDS

Affected Region	Manifestation in Patients with	
	ILS	MDS
Brain	Grade 2–4 LIS	Grade 1 LIS
Face	Bitemporal hollowing, mildly small jaw	Bitemporal hollowing, small jaw, microcephaly, tall square forehead, vertical forehead furrow, flattened midface, short upturned nose, thickened rounded upper lip, low-set posteriorly rotated ears, frontal bossing, prominent lateral nasal folds
Other	None	Cardiac defects, omphalocele, inguinal hernia, duodenal atresia, cryptorchidism, cystic kidney, pelvic kidney, polydatctyly, clinodactyly, campylodactyly, transverse palmar creases

probes (Ledbetter et al. 1989; Pilz et al. 1998*b*). In contrast, ILS may be secondary to deletions of 17p13.3, intragenic mutations, or internal deletions of the *LIS1* gene (Chong et al. 1997; Lo Nigro et al. 1997).

The precise deletion boundaries and, therefore, the deleted genes differentiating ILS from MDS in patients with 17p13.3 deletions have never been adequately determined. Previous studies have shown that the telomeric border of 17p13.3 deletions in MDS is generally more distal than those in patients with ILS (Chong et al. 1996). The study of patients with MDS and ILS also raises the question as to why patients with MDS have more severe LIS than patients with ILS. It may be assumed that the differences between the ILS and MDS phenotypes (namely, the severity of LIS and the dysmorphic features) must be secondary to deletion of additional genes telomeric to *LIS1*. Haploinsufficiency of the *LIS1* gene alone is insufficient to explain the severe (grade 1) LIS seen only in MDS patients. This suggests that there are cortical development genes other than *LIS1* deleted in patients with MDS but not in those with ILS.

The aim of this study was to investigate the genotypic difference between patients with MDS and ILS secondary to 17p13.3 deletions and to use this data to identify candidate genes to explain the difference in the phenotype. We initially performed a detailed phenotypic characterization of 34 patients with a deletion of 17p13.3, including 4 patients without LIS. We constructed a physical and transcriptional map covering the most distal 2.8 Mb of the 17p13.3 region. We used BAC/PAC genomic clones in FISH experiments to size the deletions in a spectrum of MDS and ILS patients, which defined the telomeric critical region for MDS distal to D17S1574. In addition, we mapped the 17p13.3 deletion in the four patients without LIS and mild or no dysmorphic features, to refine this region to 400 kb. Within this "telomeric MDS critical region," we used PCR analysis of somatic cell hybrids from patients with ILS and MDS to identify two candidates genes among eight, which, when deleted together with *LIS1,* could be responsible for the more severe cortical phenotype seen in MDS.

Subjects and Methods

Patient Ascertainment

Subjects were ascertained through the Lissencephaly Research Project, which currently is based at The University of Chicago, from referrals from physicians and genetic counselors, The Lissencephaly Network, and inquiry from parents of affected children. We reviewed clinical data in all 34 patients and cranial computed tomography or magnetic resonance imaging scans in 27 of 30 patients with LIS and 2 of 4 patients without LIS. If the child could not be examined, photographs were used to document the facial phenotype.

Clinical Ascertainment and Diagnosis

We selected 30 patients with ILS or MDS for study. All came to medical attention because of problems, including abnormal appearance, feeding problems, developmental delay, seizures, or a combination of these. All had LIS on brain imaging, and all had deletions of 17p13.3 by high-resolution cytogenetics or FISH. Deletions were visible in 9 of 30 patients, including 2 patients (LP90-007 and LP95-041) with unbalanced segregation of familial translocations involving chromosome 17p and 16p or 3p. Brain imaging studies were available for 27 of the 30 patients and were reviewed to confirm the diagnosis of ILS or MDS. Evaluation was performed by use of an LIS grading scale described elsewhere (Dobyns et al. 1999).

We also studied four unrelated subjects with a deletion of the 17p13.3 region but without LIS. Of these subjects, two (96.583 and 97.513) had a telomeric 17p deletion identified by cytogenetic analysis (Martin et al. 2002). The other two subjects carried a deletion of the 17p13.3 region due to an unbalanced translocation between 17p

Table 2

Primer Pairs Used to Amplify Genes Localized in the Telomeric MDS Critical Region

Gene	Forward Primer (5′→3′)	Reverse Primer (5′→3′)
ABR exon 1	GCAGTGGCTCCTTGATACAAA	AACACTATGGGCTCCACTGAG
14-3-3ε exon 6	TGGCTGCCATAGCCTAATGTA	TCAGTGACAATGGGGAGTTTC
CRK exon 2	CAGACTCCGAATAGGAGATCA	CCAAAGCCAAGGCTGTCTTGT
CRK exon 3	TAGTGGTCGTGCCTGTGTGTA	AACAGTCTGTCGCCATTTGAT
MYO1C exon 2/3	GACACTGTGTACCGAGCACTG	AGCACCGGGTTGCTCTGTAG
SKIP exon 9	CATCCTGTGGAGGCTGAAG	TACGTCATGTGGCTGCTGTAG
PITPNα 3′ UTR	AGTGGTCAACAGGAAGACCC	AATGGATCGGAACACAATGG
SREC 3′ UTR	AAGGCAGGAGGAACCTGAGTA	CAGGACAGCAGAGCAAAAGTC
RILP exon 6	AGAGGGACAGTACAAAGGGTTG	CATCAGGCTCAGCAGAATGAG
PRP8 exon 41/43	CAAGATCATGGCTGACAACC	CAAACTGCTGAATGTCAGCG
SERPINF1 exon 5	TTGACCGGAAGCATGAGTATC	GGTGACTTCGCCTTCGTAACT
RPA1 3′ UTR	CATCGGTAGGCAAAGGAAAA	ACAGAAGCCTGAAGGCAGAG
LIS1 exon 2	CATTACAGCCAAGATGGTGCT	AGCACCATCTTGGCTGTAATG

and 8p (patient DR00-063a1) or between 17p and 5p (patient DR01-001) (Mutchinick et al. 1999).

We examined 22 of the 30 patients with LIS and reviewed photographs of all but 1. We also examined and reviewed photographs of patients DR00-063a1 and DR01-001. We used a simple facial malformation grading system, in which facial changes were graded as normal (0), intermediate (1), or typical of MDS (2) by each of three experienced clinical geneticists (J.A., D.T.P., and W.B.D.). The three examiner scores were added together, giving overall scores of 0–6. Patients with scores of 0–2 were classified as having a normal facial appearance (ILS), patients with scores of 3–5 as having intermediate facial changes (ILS+), and patients with a score of 6 as having severe and characteristic facial abnormalities (MDS).

Identification and Characterization of BAC and P1-Derived Artificial Chromosomes (PAC)

Thirteen BAC clones from the RPCI-11 human library, nine BAC clones from Caltech human libraries B and D, and five PAC clones from RPCI-4 and -5 human libraries were selected to cover the most distal 3 Mb of chromosome 17p13.3, which corresponds to the presumed telomeric critical region for MDS. The vast majority of the clones were selected from human chromosome 17 database resources, such as the Sanger Institute and the Weizmann Institute, as well as genome resources, such as the National Center for Biotechnology Information (NCBI), for their content of STSs, ESTs, or genes described previously in the 17p13.3 region (Stack et al. 1995; Plummer et al. 1997; Hoff et al. 2000; McHale et al. 2000). All genomic clones were purchased from Research Genetics. Genomic DNA from BAC and PAC clones was isolated by use of an automated DNA isolation system (AutoGen 740, Integrated Separation Systems). The BACs and PACs were further characterized by PCR to analyze the presence or absence of STSs and by FISH to confirm their cytogenetic positions. Two clones, PAC95H6 and RPCI5-59D14 (GenBank AC006435), were selected on the basis of published physical and transcriptional maps of 17p13.3 (Chong et al. 1997; McHale et al. 2000), and GSS-68F18 was selected as a telomeric probe (Knight et al. 2000).

In Silico *Identification and Mapping of STSs and ESTs*

For our BAC/PAC contig, the complete or unfinished sequence for all the clones was available from the NCBI databases. We systematically analyzed these sequences to identify and map STSs and new ESTs or to confirm the mapping of known genes, using the NIX genomic sequence analysis program and the BLASTN algorithm using the NCBI databases against STS or EST databases.

STS and Gene Mapping by PCR

PCR reactions were carried out in a total volume of 50 μl containing 25–50 ng of DNA as the template, 1 × PCR buffer with 1.5 mM $MgCl_2$, 0.2 mM of each dNTP, 1 μM of each primer, and 2.5 U *Taq*Gold polymerase (PE Applied Biosystems). Amplifications were performed in a PE480 thermal cycler (Perkin Elmer-ABI), with a 5-min 94°C denaturation step followed by 35 cycles of 94°C for 35 s, 35 s of annealing at the appropriate temperature, and 40 s of elongation at 72°C. The last cycle was followed by a final extension at 72°C for 10 min. PCR products were separated on 2% agarose gels. Primer sequences and annealing temperatures for the previously assigned STSs were obtained by use of the CEPH-Généthon database, the Whitehead/MIT Center for Genome Research database, the NCBI UniSTS database, and the HUGO Genome database (GDB), as well as data published elsewhere (Hoff et al. 2000; McHale

et al. 2000). The primer pairs used to amplify all genes localized between D17S1574 and D17S1840 are listed in table 2.

FISH Analyses

Slide, probe preparation, and hybridization were completed using methods described elsewhere (Chong et al. 1997). For three-color FISH experiments, probes were directly labeled with DEAC (Diethylaminocoumarin-5-dUTP, Perkin Elmer Life Sciences), Spectrum Orange-dUTP, and Spectrum Green-dUTP (Vysis). The DEAC probe signals were pseudocolored with magenta, because of the color similarities between DEAC and DAPI. FISH slides were analyzed by use of a Zeiss Axiophot microscope with single pass filters (Chroma Technology). Images were collected using a CCD camera (Nu 200, Roper Scientific) and Smart Capture 2 software program (Digital Scientific).

Somatic Cell Hybrids

Somatic cell hybrids containing deletions of the 17p13.3 region were derived from two MDS patients (hybrid cell lines CA2 and KCB4 from patients LP82-002 and LP84-001, respectively) and from three ILS patients (hybrid lines DB, BR8, and SG2 from patients LP86-003, LP87-001, and LP90-017, respectively) and have been described elsewhere (Van Tuinen et al. 1987; Ledbetter et al. 1989; Ledbetter et al. 1992). DNA was extracted from somatic cell hybrids by use of a Puregene DNA isolation kit (Gentra Systems), according to the manufacturer's protocol. We ensured that the primers were human specific by using total genomic DNA from mouse and hamster as a negative control.

Results

Detailed Phenotypic Analysis of 34 Selected Patients

To establish a strong genotype-phenotype correlation between patients with deletions of 17p13.3, we performed a detailed phenotypic analysis on 34 selected patients (see the "Subjects and Methods" section). Among the 34 patients, by comparison with normal MRI images (fig. 1*I* and 1*J*), 30 patients had LIS and 4 had no LIS. Of the 30 patients with LIS, 10 had consensus ILS with a normal facial appearance, except for the minor changes typical of this condition (table 1; fig. 1*A*); 9 patients had intermediate facial abnormalities and were classified as ILS+ (fig. 1*C*); and 11 had a consensus MDS facial appearance (table 1 and fig. 1*E* and 1*G*). Patients with ILS always had LIS grade 3 or 4 (fig. 1*B*), whereas those with ILS+ had LIS grade 2 or 3 (fig. 1*D*). In contrast, all patients with consensus MDS had LIS grade 1 or diffuse agyria (fig. 1*F* and 1*H*) and the characteristic facial features (table 1). Thus, we found a strong correlation between the most prominent dysmorphic features and most severe brain abnormalities.

Of the four subjects who did not have LIS, two (96.583 and 97.513) were phenotypically normal (Martin et al. 2002), and the other two (DR00-063a1 and DR01-001) were mentally retarded. Regarding the latter, DR00-063a1 had a normal MRI scan, and DR01-001 had epilepsy and microcephaly, with an MRI scan showing a thin corpus callosum and frontal lobe hypoplasia (fig. 1*L*). DR01-001 had mild facial dysmorphism and has been reported elsewhere (Mutchinick et al. 1999) as having a facial phenotype consistent with MDS (fig. 1*K*). On consensus review for this study, we concluded that she had an abnormal facial appearance that did not meet our criteria for typical MDS.

Physical and Transcriptional Map from D17S1845 to the 17p Telomere

To identify which telomeric genes could participate with *LIS1* in producing the more severe phenotype seen in MDS, compared to that in ILS, we constructed a physical and transcriptional map from the proximal marker D17S1845 (close to *LIS1*) toward the telomere. A BAC/PAC contig was created by linking newly characterized BAC and PAC clones obtained from numerous databases with data published elsewhere (see the "Subjects and Methods" section). We used an STS-based approach combined with computational methods to construct a BAC/PAC contig spanning ~2.8 Mb (fig. 2). Each BAC or PAC clone was tested by FISH analysis on normal human metaphase chromosomes to verify its unique localization to 17p13.3. BAC407I21 (GenBank accession number AF322450), for which sequence is available at the NCBI database, was previously mapped on 17p13.3 by Gu and colleagues (Shanghai Cancer Institute).

The completed contig consists of 23 BAC and 6 PAC clones (fig. 2). It includes three regions covered only by a single BAC clone, which corresponds to the clones RPCI-11 135N5 (GenBank accession number AC015799), RPCI-11 676J12 (GenBank AC087392), and RPCI-11 818O24 (GenBank AC032044). For the latter region, the *CRK* gene (GenBank NM_005206 and NM_016823) helped us to link the clone RPCI11-818O24 with BAC407I21. The overlap between these two BACs, not previously identified as being overlapping clones, corresponds to exon 2 and intron 2 of the highly conserved *CRK* gene, which we estimate to be at least 12 kb by comparison with the mouse genome sequence (cf. clone RPCI23-78H4 [GenBank AL669897] and clone RPCI23-190H20 [GenBank AL663094]). In addition, the telomeric minicontig could not be joined with the main contig (fig. 2). On the basis of the size estimation of this region by the Weizmann Institute database, we expect that the gap between PAC RPCI5-

1029F21 (GenBank AC015853) and BAC CTD-2578J3 (GenBank AC108006) is no more than 150 kb in length. Using the physical clone contig as a resource, we assigned 23 known genes, 11 ESTs or unknown genes, and 1 pseudogene to17p13.3, all of which were described in the Unigene database. We also assigned 24 genetic markers or anonymous STSs and 15 BAC/PAC end clones to this region (fig. 2).

Characterization of the "Telomeric Critical Region for MDS"

To further define the "telomeric MDS critical region," we used a selection of BAC/PAC clones from our map as probes (fig. 2, clones noted in red) for FISH analysis to size and determine the boundaries of the deletion in our 34 selected patients (fig. 3). In addition, we used two BACs centromeric to D17S1845 as controls: RPCI11-713H12 (AC025518) contains the *NUDEL* gene (NM_030808), which interacts with LIS1 (Sasaki et al. 2000), and was not deleted in any of the 34 patients (fig. 3). Probe RPCI11-305G1 (AC032038) contains the *profilin1* gene (NM_005022) and was deleted in only 4 of 34 patients (fig. 3). For one patient with MDS (LP84-001), PAC95H6 showed partial deletion of the *LIS1* gene (fig. 3), which was confirmed by deletion of the telomeric overlapping clone RCPI11-135N5, which contains exons 1 and 2 of the *LIS1* gene (data not shown). Comparing the size of the deletions identified in patients with MDS with the size of the deletions in patients with ILS + and ILS, we found that BAC RPCI11-107N19 (AC006405) was deleted in three patients with ILS+ (LR01-118, LP99-086, and LP86-003) and all patients with MDS (fig. 3). Next, we compared the size of the deletion among patients with MDS and found that, for one MDS patient (LP82-002), the deletion did not extend beyond BAC RPCI11-818O24 (figs. 2 and 3). Therefore, our FISH studies demonstrated that the "telomeric critical region for MDS" is contained within the two BACs RPCI11-107N19 and RPCI11-818O24, which means that the critical region is distal to D17S1574, which is contained in RPCI11-4F24 (AC007873), and proximal to D17S1582, which is located at the telomeric end of RPCI11-818O24 (figs. 2 and 3).

This result is also supported by sizing of the deletion in the four subjects who did not have LIS. For the two phenotypically normal individuals (96.583 and 97.513), FISH analysis revealed a deletion of the 17p telomeric region, which for 97.513 included the *ABR* gene (fig. 3). Our data confirmed the previous cytogenetic analysis (Martin et al. 2002), which revealed satellites on the short arm of one chromosome 17 and indicated that the most distal genes are not dosage sensitive. Next, we mapped the breakpoint on the deleted chromosome 17 of the two mentally retarded patients (see the "Subjects and Methods" section) as being around marker SHGC-32238 for patient DR00-063a1 and D17S1574 for DR01-001 (figs. 2 and 3). DR00-063a1, with the smallest deletion, had mild mental retardation and normal facial appearance, as did her mother (data not shown). DR00-001, with the largest deletion, had severe mental retardation and mild facial dysmorphism not considered typical of MDS (fig. 1*K* and 1*L*). However, patient DR01-001 also has several specific phenotypic traits characteristic of the 5p trisomy due to significant additional material added to the deleted 17p as a result of the translocation with 5p. Specific phenotypic characteristics of the trisomy 5p present in patient DR01-001 are a depressed nasal bridge, long fingers, and bilateral talipes equinovarus (Mutchinick et al., 1999). In these two patients, we identified a region that may contain a gene involved or responsible for mental retardation, which seems to overlap with the "telomeric critical region for MDS" previously defined.

Finally, this data has enabled us to design a three-color FISH assay using PAC95H6, BAC RPCI11-818O24, and BAC68F18 (fig. 3) as a diagnostic screen for patients with 17p13.3 deletions, and the results showed a robust correlation with the clinical phenotype (fig. 4). Deletion of PAC 95H6 alone (fig. 4*B*) was associated with ILS (fig. 1*C* and 1*D*). Deletion of PAC95H6 in combination with one or both of RPCI11-818O24 or BAC68F18 (fig. 4*C*) was associated with MDS (fig. 1*G* and 1*H*). Deletion of RPCI11-818O24 and BAC68F18 but not PAC95H6 (fig. 4*D*) was not associated with a LIS phenotype (fig. 1*K* and 1*L*).

Deletion of CRK *and* 14-3-3ε *Is Seen Only in Patients with the Most Severe Form of LIS*

With the telomeric MDS critical region defined, we wanted to determine which genes within that region (in addition to *LIS1*) may contribute to the MDS phenotype when deleted. We used somatic cell hybrids established from five selected patients with LIS and deletions involving the telomeric MDS critical region. Among these five patients, three had an intermediate ILS+ phenotype with mild dysmorphic features and grade 3 LIS for SG2 (LP90-017) or grade 2 LIS for BR8 (LP87-001) and DB (LP86-003). The two others, CA2 (LP82-002) and KCB4 (LP84-001) had a consensus MDS phenotype with distinct dysmorphic features and grade 1 LIS (fig. 3).

By PCR, we tested all known genes in the telomeric MDS critical region between D17S1574 and D17S1582 (fig. 2 and table 2) (see the "Subjects and Methods" section). PCR results showed that, for hybrid SG2, amplification of the *PRP8* gene (GenBank XM_028335) delineated a telomeric deletion boundary around the STS marker SHGC-32238 (figs. 2 and 5). For hybrids BR8

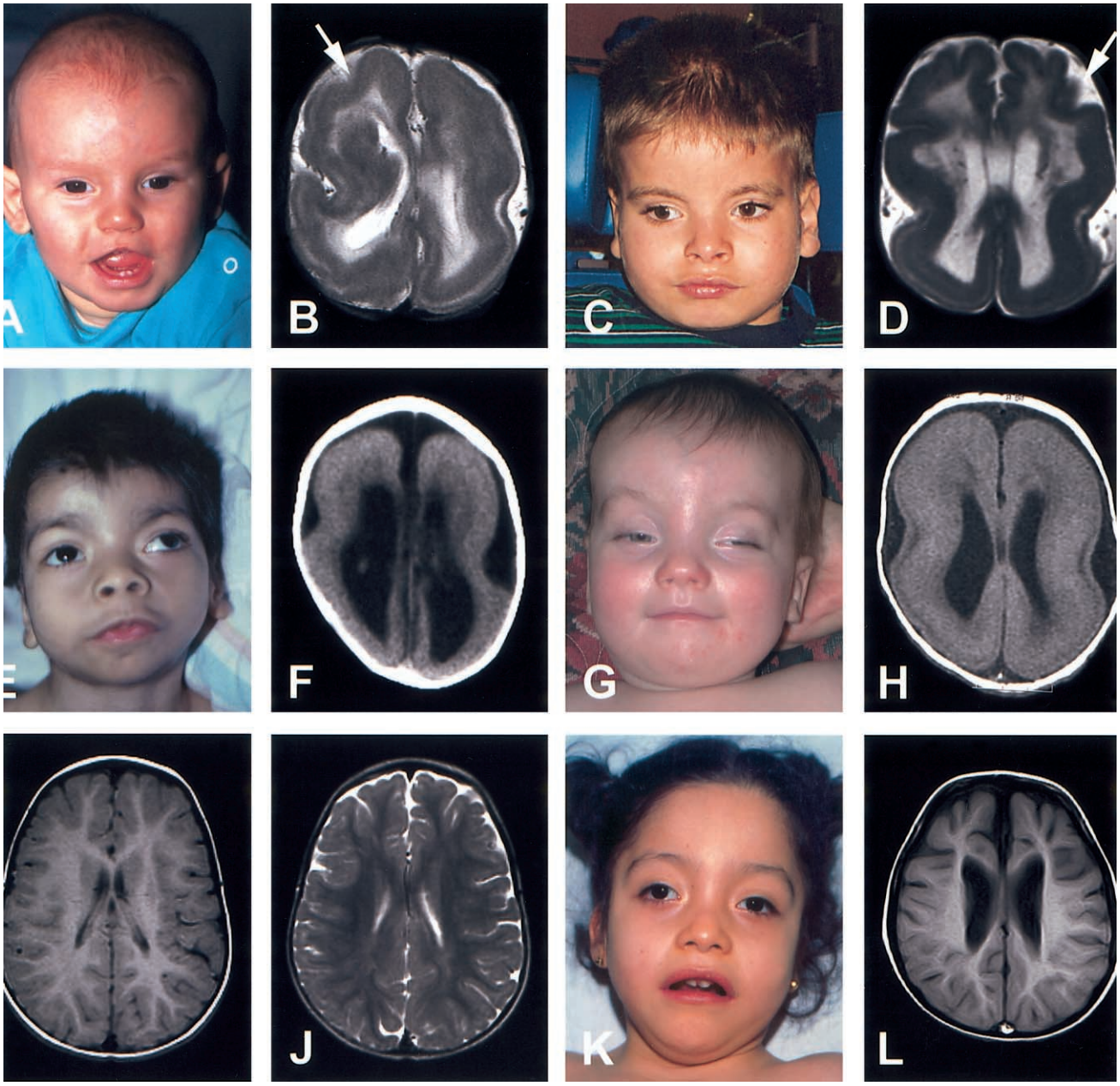

Figure 1 Detailed phenotypic analysis of patients with deletions of 17p13.3, showing increasing severity of brain and face changes with larger deletions extending closer to the 17p telomere. LP95-108 has typical ILS with normal facial appearance (*A*) and LIS grade 3 with a posterior > anterior gradient (*B*) associated with a small submicroscopic deletion. LP99-086 has ILS with facial changes intermediate between typical ILS and MDS (*C*) and LIS grade 3 with a posterior > anterior gradient (*D*). LP82-002 (*E* and *F*) and LR01-167 (*G* and *H*) have consensus MDS (*E* and *G*) and severe LIS grade 1 (*F* and *H*) with no visible gradient. Both the brain and face abnormalities are more severe than in the patients with ILS shown (*A–D*). Normal T1 and T2 axial images are shown for comparison (*I* and *J*). The face and brain abnormalities are more subtle in subjects with deletions that do not include the *LIS1* gene. DR01-001 has a mildly dysmorphic facial appearance not specific for MDS (*K*) and mild frontal lobe hypoplasia without LIS (*L*).

and DB, their telomeric breakpoints are respectively localized between the *SREC* (GenBank XM_008489) and *PITPNα* (GenBank NM_006224) genes close to D17S1577 and between the *MYO1C* (GenBank XM_028385) and *CRK* genes (figs. 2 and 5). Finally, deletions in hybrids CA2 and KCB4 probably have the same telomeric boundary, which is localized around D17S1582, shown by amplification of only the *ABR* gene (NM_021962 and NM_001092) for both patients (figs. 2 and 5). In addition, for KCB4, we confirmed the partial de-

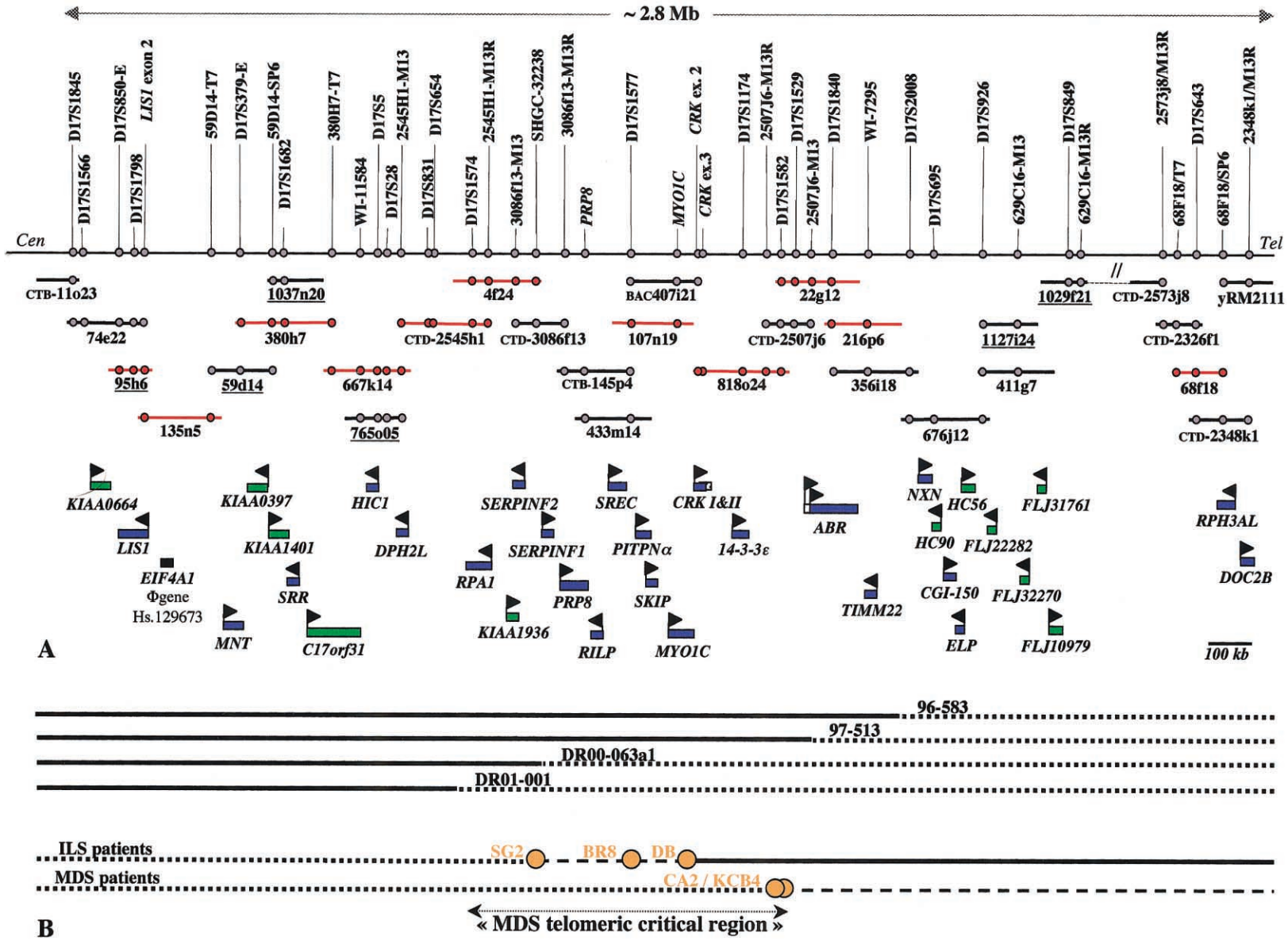
~ 2.8 Mb
Cen
Tel
D17S1845
D17S1566
D17S850-E
D17S1798
LIS1 exon 2
59D14-T7
D17S379-E
59D14-SP6
D17S1682
380H7-T7
WI-11584
D17S5
D17S28
2545H1-M13
D17S831
D17S654
D17S1574
2545H1-M13R
3086f13-M13
SHGC-32238
3086f13-M13R
PRP8
D17S1577
MYO1C
CRK ex. 2
CRK ex.3
D17S1174
2507J6-M13R
D17S1582
D17S1529
2507J6-M13
D17S1840
WI-7295
D17S2008
D17S695
D17S926
629C16-M13
D17S849
629C16-M13R
2573j8/M13R
68F18/T7
D17S643
68F18/SP6
2348k1/M13R
CTB-11o23
1037n20
4f24
BAC407i21
22g12
1029f21
CTD-2573j8
yRM2111
74e22
380h7
CTD-2545h1
CTD-3086f13
107n19
CTD-2507j6
216p6
1127i24
CTD-2326f1
95h6
59d14
667k14
CTB-145p4
818o24
356i18
411g7
68f18
135n5
765o05
433m14
676j12
CTD-2348k1
KIAA0664
LIS1
EIF4A1
Φgene
Hs.129673
KIAA0397
KIAA1401
SRR
MNT
C17orf31
HIC1
DPH2L
SERPINF2
SERPINF1
RPA1
PRP8
KIAA1936
SREC
PITPNα
SKIP
RILP
MYO1C
CRK I&II
14-3-3ε
ABR
TIMM22
NXN
HC56
HC90
FLJ22282
CGI-150
FLJ32270
ELP
FLJ10979
FLJ31761
RPH3AL
DOC2B
100 kb
A
96-583
97-513
DR00-063a1
DR01-001
ILS patients
MDS patients
SG2
BR8
DB
CA2 / KCB4
« MDS telomeric critical region »
B

letion of the LIS1 gene by no amplification of exon 2 (data not shown). Thus, in patients defined as having an MDS phenotype with the most severe LIS grade (CA2 and KCB4), we found exclusive deletion of only two genes (*CRK* and *14-3-3ε*) that were not deleted in ILS+ patients (SG2, BR8, and DB) (fig. 5).

Discussion

Several syndromes—such as Williams syndrome (del 7q11), Prader-Willi and Angelman syndromes (del 15q11-q13), and DiGeorge syndrome (del 22q11)—are associated with hemizygous deletions at recurrent sites of a specific chromosome (Morrow et al. 1995; Osborne et al. 1997; Christian et al. 1999). These are classical contiguous gene-deletion syndromes, in which the inactivation of several unrelated genes is involved in producing a complex phenotype. MDS has long been recognized as a contiguous gene-deletion syndrome with variable breakpoints, but the relationship between the genes deleted within chromosome 17p13.3 and the MDS phenotype has never been elucidated. By mapping the extent of deletions of the 17p13.3 region, which result in either ILS or MDS, we previously described a common critical region containing the *LIS1* gene responsible for both disorders (Chong et al. 1997). Our previous data also suggested that considerable overlap exists between the deleted region in patients with ILS and MDS, with the deletion in patients with MDS extending more telomeric on 17p13.3 (Ledbetter et al. 1989; Chong et al. 1997).

We have previously shown a relationship between genotype and phenotype in a large number of patients with ILS secondary to intragenic *LIS1* abnormalities, revealing a correlation between LIS severity and the location and type of *LIS1* mutation (Cardoso et al. 2000; Leventer et al. 2001). In that group of patients—even in those with a completely deleted or nonfunctional *LIS1* gene—there were areas of simplified brain folds (pachygyria), rather than completely absent folds (agyria), as seen only in patients with MDS. There has never been an adequate explanation as to why patients with MDS have the most severe LIS phenotype. One hypothesis is that they are hemizygous for one or more genes, other than *LIS1*, that are involved in cortical development. To address this question, we initially constructed a detailed physical and transcriptional map of the 17p13.3 region. Next, we used this map to compare and contrast the boundaries of the deletions in a large number of patients with ILS and MDS. In addition, we studied four patients with terminal deletions involving 17p13.3 but without LIS. As hypothesized, we have shown that patients with MDS have a larger telomeric deletion than patients with ILS, and the larger deletions show a more severe grade of LIS. We have also shown that a deletion from *ABR*, toward the telomeric end of chromosome 17p, is associated with no apparent phenotype. These data proved very helpful in allowing us to define the distal boundary of the telomeric MDS critical region. We were able to narrow this region to 400 kb by comparing the deletions in ILS and MDS patients. In this interval we identified eight genes deleted exclusively in patients with MDS. These data clearly suggest that genes other than *LIS1* may participate in producing the MDS phenotype and support for the first time the concept that MDS truly is a contiguous gene-deletion syndrome.

The identification of eight genes (*PRP8, RILP, SREC, PITPNα, SKIP, MYO1C, CRK,* and *14-3-3ε*) in our newly defined telomeric MDS critical region is a first step in our goal to characterize which additional genes distal to *LIS1* may be responsible for the clinical features that distinguish MDS from ILS. Existing functional information regarding the proteins encoded by these genes show that PRP8 is a highly conserved spliceosomal protein, which provides important catalytic and regulatory functions for pre-mRNA processing (Kuhn et al. 1999). Rab7-interacting lysosomal protein (or RILP) controls lysosomal transport by inducing the recruitment of functional dynein-dynactin motor complexes (Jordens et al. 2001). The scavenger receptor expressed by endothelial cells (or SREC) mediates the selective uptake of modified low-density lipoprotein (LDL) such as acetylated-LDL and oxidized-LDL into endothelial cells (Adachi et al. 2002). Phosphatidylinositol transfer protein alpha (PITPNα) is a member of a diverse set of

Figure 2 Physical and transcriptional map of the interval from D17S1845 to the telomere. *A,* The chromosomal orientation of the BAC/PAC contig covering the most distal 2.8 Mb of chromosome 17 in the region p13.3 is indicated. STS markers, genes, and BAC ends used for mapping are depicted by vertical lines at the top of the figure. A gray or red circle signifies the presence of an STS, a gene, or a BAC end on an individual PAC or BAC clone. All PAC clones are underlined, and BAC clones used in FISH analysis are indicated in red. The broken line indicates the gap between the main contig and the telomeric minicontig. Known genes mapped previously in this region are noted in blue, and the direction of transcription is indicated by an arrow. A pseudogene is denoted by a black box. The cDNA clones corresponding to unknown genes are noted in green. All known and new genes are placed exactly below the genomic clones that contain them. *B,* Schematic representation of deletions of the 17p13.3 region identified in patients with ILS, MDS, or other phenotypes without LIS. The solid lines below the map represent nondeleted genomic BAC/PAC clones. The dotted lines represent deletions associated with the patient number listed above. For patients with ILS or MDS, the dashed line indicates the largest deletion identified in each group of patients. The telomeric boundaries of 17p13.3 deletion of hybrids SG2, BR8, DB, CA2, and KCB4 are indicated by orange circles.

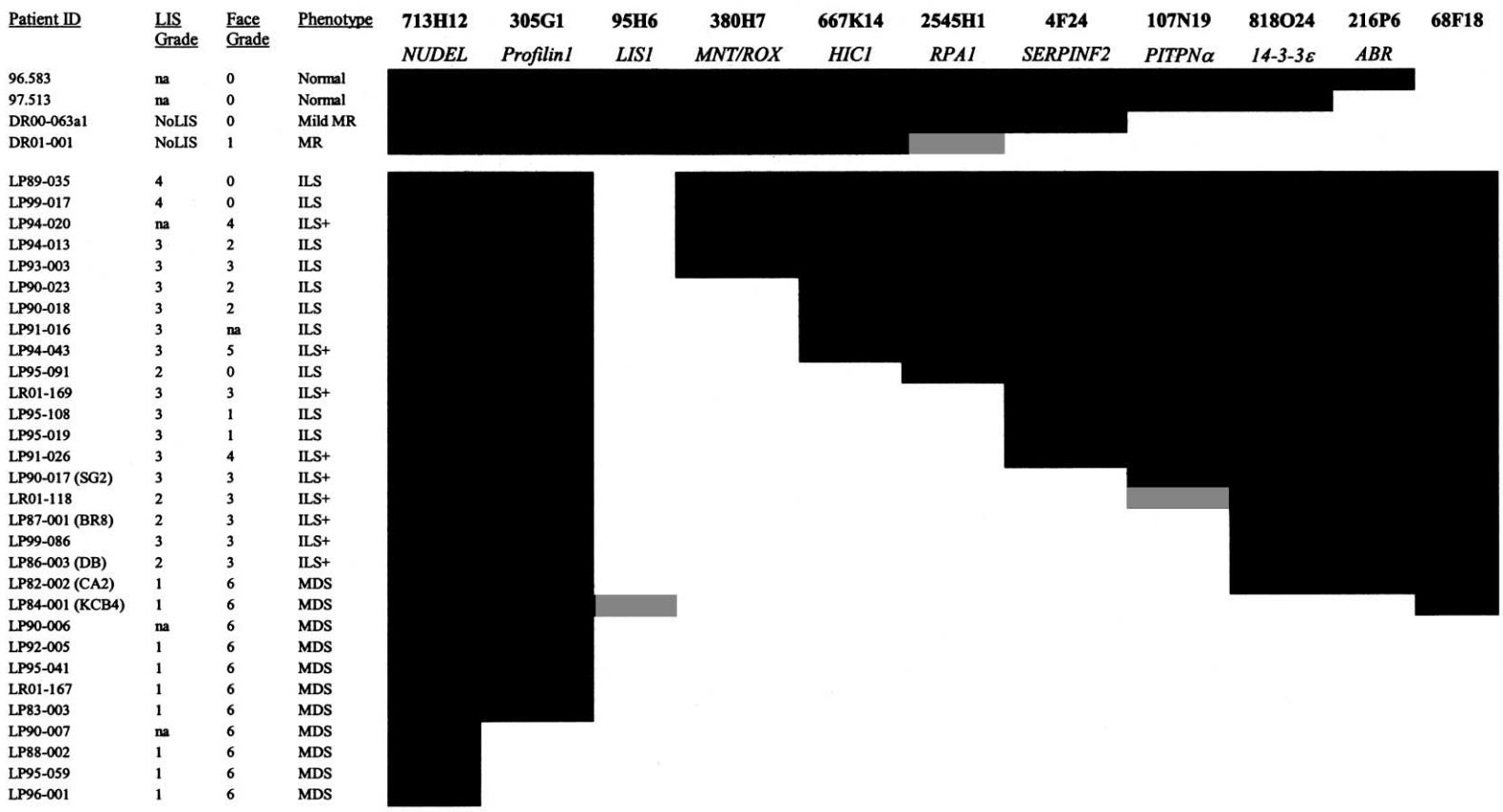

Figure 3 Extent of deletion in 12 patients with MDS, 18 patients with ILS, and 4 patients without LIS. Black boxes denote the presence of the probe on both copies of chromosome 17, and white boxes denote the presence of the probe on only one chromosome 17. Gray boxes denote a partial deletion of the probe on one chromosome 17. na = Data not available. BAC ID numbers (*boldface*) and gene symbols (*italics*) are listed across the top of the figure from centromere (*left*) to telomere (*right*).

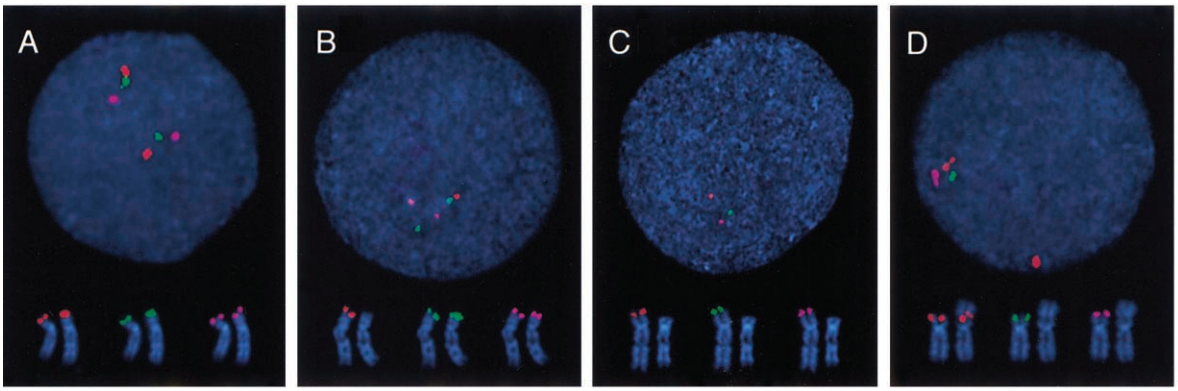

Figure 4 Three-color FISH analysis showing the variability of the deletions of the 17p13.3 region. Three probes—PAC95H6 (*red*), BAC818O24 (*green*), and BAC68F18 (*magenta*)—from the 17p subtelomeric region were used in these FISH experiments to size the deletion of the 17p13.3 region in various patients (*B*, *C*, and *D*) compared with a normal control (*A*). *B*, FISH on patient (LP99-086) who has ILS (fig. 1*C* and 1*D*) showed the absence of PAC95H6 in red (containing the *LIS1* gene). *C*, In patient LR01-167, who has MDS (fig. 1*G* and 1*H*), there is absence of signal of all three probes on one chromosome 17. *D*, Patient DR01-001 does not have all typical MDS facial features or LIS, but does have an abnormal brain MRI (frontal lobe hypoplasia and partial agenesis of the corpus callosum) (fig. 1*K* and 1*L*). Her FISH study shows the presence of PAC95H6 on both chromosome 17s and absence of the probes BAC818O24 and BAC68F18 from one chromosome 17.

cytosolic phospholipid transfer proteins that are distinguished by their ability to regulate the interface between signal transduction, membrane-trafficking, and lipid metabolic pathways in eukaryotic cells (Liscovitch and Cantley 1995). SKIP (Ski-interacting protein) is a partner of the oculopharyngeal muscular dystrophy gene *PABP2* and stimulates directly or indirectly muscle-specific gene expression (Kim et al. 2001). MYO1C is a motor protein and participates in the slow component of adaptation by hair cells, which are the sensory cells of the inner ear (Holt et al. 2002). The *CRK* gene exists in two splice variants, *CRK I* (28 kDa) and *CRK II* (42 kDa), of which *CRK II* encodes an additional N-terminal SH3 domain (Reichman et al. 1992). The product of *CRK* is an adaptator signaling protein that is mostly composed of SH2 and SH3 domains, and has been shown to play a pivotal role in cell proliferation, differentiation, and migration (Feller et al. 1998). The 14-3-3ε protein is a member of a large family of signaling molecules defined as discrete phosphoserine/threonine binding modules. The 14-3-3 family of proteins play critical roles in cell signaling events that control progress through the cell cycle, transcriptional alterations in response to environmental cues, and programmed cell death (Yaffe et al. 2002).

On the basis of this functional data, many of these genes may be considered good candidates to be involved in the more severe phenotype seen in patients with MDS. Our PCR mapping results of somatic cell hybrids from patients with MDS who have interstitial deletions has allowed us to further reduce the number of candidate genes likely to be involved in the brain phenotype MDS. When we compared the severity of LIS in the patients in this study, only those with MDS had complete agyria (grade 1). We know from previous studies that deletion of *LIS1* alone is not sufficient to cause this severe form of LIS (Cardoso et al. 2000). The patients in our study with complete agyria uniformly had the largest deletions (fig. 3). Gene-by-gene mapping of these deletions in selected patients by PCR showed that two genes (*CRK* and *14-3-3ε*) were exclusively deleted only in those patients with the most severe form of LIS (fig. 5). Thus, we conclude that deletion of one or both of these genes in addition to *LIS1* may contribute to the severe LIS phenotype seen only in MDS. To take this hypothesis further, it must then be assumed that one of these genes has a role in cortical development and specifically in neuronal migration.

The *14-3-3ε* gene product is probably the best candidate, on the basis of a mouse knock-out phenotype that supports a role for *14-3-3ε* in cortical development (K. Toyo-oka, A. Shionoya, M. J. Gambello, C. Cardoso, R. J. Leventer, H. L. Ward, R. Ayala, L. H. Tsai, W. B. Dobyns, D. H. Ledbetter, S. Hirotsune, and A. Boris-Wynshaw, unpublished data). As in human, heterozygous loss of both *Lis1* and *14-3-3ε* result in more severe cortical and hippocampal developmental defects (Hirotsune et al. 1998; Toyo-oka et al., unpublished data). Thus, the phenotypes in both human and mouse support the hypothesis that *14-3-3ε* is a gene that may contribute to the severe migration defects seen in patients with MDS. *CRK* should also be considered as a candidate to participate in the LIS phenotype seen in MDS. It has been shown that *CRK* may have a role in

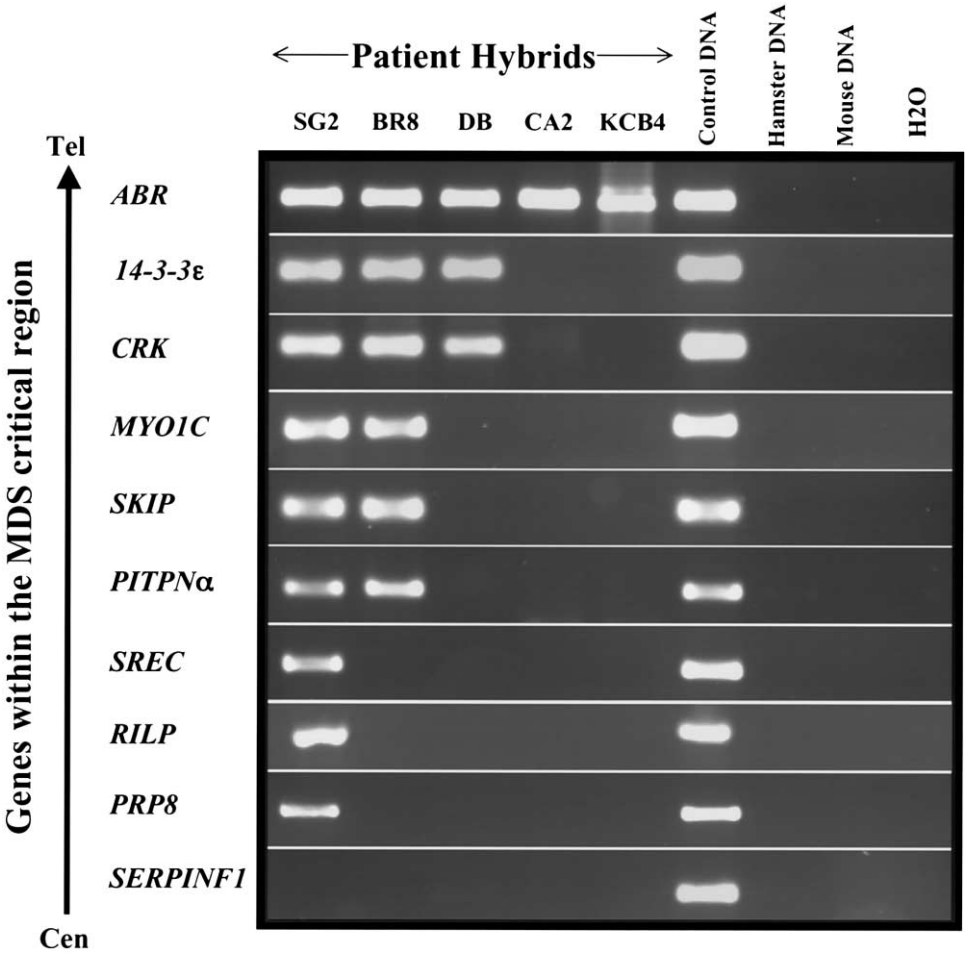

Figure 5 Extent of deletion in the telomeric MDS critical region. PCR analysis was performed on somatic cell hybrid cell lines derived from lymphoblasts of three patients with ILS—SG2 (LP90-017), BR8 (LP87-001), and DB (LP86-003)—and from two patients with MDS—CA2 (LP82-002) and KCB4 (LP84-001)—whose deletion breakpoints have been characterized by FISH analysis. Primers used specially amplified all 10 human genes (see the "Subjects and Methods" section) that extend from the centromere (SERPINF1) to telomere (ABR) that are present within the telomeric MDS critical region. DNAs from hamster, mouse, and human were used in these experiments to show the specificity of the primers.

cell proliferation and migration by regulating the connection between integrins and the cellular cytoskeleton in areas named "focal adhesion" (Tsuda et al. 2002). However, even if *CRK* is involved in cell growth and motility, there is no evidence as yet that haploinsufficiency of this gene can cause a brain anomaly, and the creation of a mouse knockout of the *CRK* gene is required. In view of the lack of functional information on the *CRK* gene, and evidence that *14-3-3ε* is involved in brain development, we propose that, of these two genes, *14-3-3ε* is the better candidate for the more severe LIS phenotype seen in patients with MDS compared with patients with ILS.

In conclusion, we propose that MDS is truly a contiguous gene-deletion syndrome, caused by haploinsufficiency of at least nine critical genes, including *LIS1,* that contribute to the facial and brain phenotype seen in patients with MDS. Furthermore, we suggest that the deletion of *14-3-3ε* and/or *CRK* in addition to *LIS1* is the factor responsible for the most severe form of classical LIS seen only in patients with MDS.

Acknowledgments

We would like to thank the patients, their families, and their physicians who referred them for study. We gratefully acknowledge the help of Dr. Akira Tanigami, Patti Mills, Albert Leung, Anthony Bodin, Dr. Andrew Wong, and Dr. J. L. Ceballos. This work was supported in part by grants from the National Institutes of Health (PO1 NS39404, to W.B.D. and D.H.L., and 1 RO1 HD36715-03, to D.H.L.), the Lissencephaly Network, and the March of Dimes (6-FY00-404, to D.H.L. and C.L.M.). C.C. is supported by an INSERM Fel-

lowship and the David and Janice Katz Fellowship in Human Genetics.

Electronic-Database Information

Accession numbers and URLs for data presented herein are as follows:

CEPH-Généthon Database, http://www.cephb.fr/

GenBank, http://www.ncbi.nlm.nih.gov/entrez/, (for RPCI4-765O05 [accession no. AL137038], RPCI5-59D14 [accession no. AC006435], RPCI5-1029F21 [accession no. AC015853], RPCI5-1037N22 [accession no. AL450226], RPCI5-1127L24 [accession no. AC008087], RPCI11-4F24 [accession no. AC007873], RPCI11-22G12 [accession no. AC016292], RPCI11-74E22 [accession no. AC005696], RPCI11-107N19 [accession no. AC006405], RPCI11-135N5 [accession no. AC015799], RPCI11-216P6 [accession no. AC015884], RPCI11-356I18 [accession no. AC036164], RPCI11-380H7 [accession no. AC021705], RPCI11-411G7 [accession no. AC027455], RPCI11-433M14 [accession no. AC068936], RPCI11-667K14 [accession no. AC090617], RPCI11-676J12 [accession no. AC087392], RPCI11-818O24 [accession no. AC032044], CTB-11O23 [accession no. AC002316], BAC407I21 [accession no. AF322450], CTB-145P4 [accession no. AC002093], CTD-2326F1 [accession no. AC109339], CTD-2348K1 [accession no. AC108004], CTD-2507J6 [accession no. AC107911], CTD-2545H1 [accession no. AC099684], CTD-2573J8 [accession no. AC108006], CTD-3086F13 [accession no. AC099721] and yRM2111 (17pTEL) [accession no. AF240580], RPCI23-78H4 [accession no. AL669897], RPCI23-190H20 [accession no. AL663094], RPCI11-305G1 [accession no. AC032038], RPCI11-713H12 [accession no. AC025518], *NUDEL* [accession no. NM_030808], *profilin1* [accession no. NM_005022], *KIAA0664* [accession no. XM_03478], *LIS1* [accession no. XM_034770], *MNT* [accession no. XM_012601], *SRR* [accession no. NM_021947], *KIAA0397* [accession no. AB007857], *C17orf31* [or KIAA0732] [accession no. XM_029470], KIAA1401 [accession no. AB037822], *HIC1* [accession no. NM_006497], *DPH2L* [accession no. NM_001383], *RPA1* [accession no. NM_002945], *SERPINF2* [accession no. NM_000934], *SERPINF1* [accession no. NM_002615], *KIAA1936* [accession no. XM_056082], *PRP8* [accession no. XM_028335], *RILP* [accession no. NM_031430], *SREC* [accession no. XM_008489], *PITPN-α* [accession no. NM_006224], *SKIP* [accession no. NM_016532], *MYO1C* [accession no. XM_028385], *CRK III* [accession no. NM_005206 and NM_016823], *14-3-3ϵ* [accession no. NM_006761], *ABR* [accession no. NM_021962 and NM_001092], *TIMM22* [accession no. XM_033715], *NXN* [accession no. XM_033714], *HC90* [accession no. AF177344], *CGI-150* [accession no. NM_016080], *ELP* [accession no. AF229804], HC56 [accession no. AF177341], FLJ22282 [accession no. NM_024792], *FLJ32270* [accession no. AK056832], *FLJ10979* [accession no. NM_018289], *FLJ31761* [accession no. AK056323], *RPH3AL* [accession no. NM_006987], and *DOC2B* [accession no. NM_003585])

HUGO chromosome 17, http://gdbwww.gdb.org/hugo/chr17/

Lissencephaly Network, http://www.lissencephaly.org

NCBI UniGene, http://www.ncbi.nlm.nih.gov/UniGene/

NCBI UniSTS, http://www.ncbi.nlm.nih.gov:80/entrez/query.fcgi?CMD=DB=UniSts

NIX application, http://www.hgmp.mrc.ac.uk/Registered/Webapp/nix/

Online Mendelian Inheritance in Man (OMIM), http://www.ncbi.nlm.nih.gov/Omim/ (for MDS, PAFAH1B1/LIS1, and DCX)

Sanger Institute, http://www.ensembl.org/Homo_sapiens/

Weizmann Institute, http://bioinformatics.weizmann.ac.il/chr17/

Whitehead Institute, http://www-genome.wi.mit.edu/cgi-bin/contig/sts_by_chrom?chrom=Chr17

References

Adachi H, Tsujimoto M (2002) Characterization of human gene encoding scavenger receptor expressed by endothelial cells (SREC) and its regulation by a novel transcription factor, endothelial zinc finger protein-2 (EZF-2). J Biol Chem 277:24014–24021

Cardoso C, Leventer RJ, Matsumoto N, Kuc JA, Ramocki MB, Mewborn SK, Dudlicek LL, May LF, Mills PL, Das S, Pilz DT, Dobyns WB, Ledbetter DH (2000) The location and type of mutation predict malformation severity in isolated lissencephaly caused by abnormalities within the *LIS1* gene. Hum Mol Genet 9:3019–3028

Chong SS, Tanigami A, Roschke AV, Ledbetter DH (1996) 14-3-3 epsilon has no homology to LIS1 and lies telomeric to it on chromosome 17p13.3 outside the Miller-Dieker syndrome chromosome region. Genome Res 6:735–741

Chong SS, Pack SD, Roschke AV, Tanigami A, Carrozzo R, Smith AC, Dobyns WB, Ledbetter DH. (1997) A revision of the lissencephaly and Miller-Dieker syndrome critical regions in chromosome 17p13.3. Hum Mol Genet 6:147–155

Christian, SL, Fantes JA, Mewborn SK, Huang B, Ledbetter DH (1999) Large genomic duplicons map to sites of instability in the Prader-Willi/Angelman syndrome chromosome region (15q11–q13). Hum Mol Genet 8:1025–1037

Dobyns, WB, Curry CJ, Hoyme HE, Turlington L, Ledbetter DH (1991) Clinical and molecular diagnosis of Miller-Dieker syndrome. Am J Hum Genet 48:584–594

Dobyns WB, Reiner O, Carrozzo R, Ledbetter DH (1993) Lissencephaly: a human brain malformation associated with deletion of the *LIS1* gene located at chromosome 17p13. JAMA 270:2838–2842

Dobyns WB, Truwit CL, Ross ME, Matsumoto N, Pilz DT, Ledbetter DH, Gleeson JG, Walsh CA, Barkovich AJ (1999) Differences in the gyral pattern distinguish chromosome 17-linked and X-linked lissencephaly. Neurology 53:270–277

Feller SM, Posern G, Voss J, Kardinal C, Sakkab D, Zheng J, Knudsen BS (1998) Physiological signals and oncogenesis mediated through Crk family adapter proteins. J Cell Physiol 177:535–552

Hirotsune S, Fleck MW, Gambello MJ, Bix GJ, Chen A, Clark GD, Ledbetter DH, McBain CJ, Wynshaw-Boris A (1998) Graded reduction of Pafah1b1 (Lis1) activity results in neuronal migration defects and early embryonic lethality. Nat Genet 19:333–339

Hoff C, Seranski P, Mollenhauer J, Korn B, Detzel T, Reinhardt R, Ramser J, Poustka A (2000) Physical and transcriptional mapping of the 17p13.3 region that is frequently deleted in human cancer. Genomics 70:26–33

Holt JR, Gillespie SK, Provance DW, Shah K, Shokat KM, Corey DP, Mercer JA, Gillespie PG (2002) A chemical-genetic strategy implicates myosin-1c in adaptation by hair cells. Cell 108:371–381

Jordens I, Fernandez-Borja M, Marsman M, Dusseljee S, Janssen L, Calafat J, Janssen H, Wubbolts R, Neefjes J (2001) The Rab7 effector protein RILP controls lysosomal transport by inducing the recruitment of dynein-dynactin motors. Curr Biol 11:1680–1685

Kim YJ, Noguchi S, Hayashi YK, Tsukahara T, Shimizu T, Arahata K (2001) The product of an oculopharyngeal muscular dystrophy gene, poly(A)-binding protein 2, interacts with SKIP and stimulates muscle-specific gene expression. Hum Mol Genet 10:1129–1139

Knight SJ, Lese CM, Precht KS, Kuc J, Ning Y, Lucas S, Regan R, Brenan M, Nicod A, Lawrie NM, Cardy DL, Nguyen H, Hudson TJ, Riethman HC, Ledbetter DH, Flint J (2000) An optimized set of human telomere clones for studying telomere integrity and architecture. Am J Hum Genet 67:320–332

Kuhn AN, Li Z, Brow DA (1999) Splicing factor Prp8 governs U4/U6 RNA unwinding during activation of the spliceosome. Mol Cell 3:65–75

Ledbetter DH, Ledbetter SA, vanTuinen P, Summers KM, Robinson TJ, Nakamura Y, Wolff R, White R, Barker DF, Wallace MR, Collins FS, Dobyns WB (1989) Molecular dissection of a contiguous gene syndrome: frequent submicroscopic deletions, evolutionarily conserved sequences, and a hypomethylated "island" in the Miller-Dieker chromosome region. Proc Natl Acad Sci USA 86:5136–5140

Ledbetter SA, Kuwano A, Dobyns WB, Ledbetter DH (1992) Microdeletions of chromosome 17p13 as a cause of isolated lissencephaly. Am J Hum Genet 50:182–189

Leventer RJ, Cardoso C, Ledbetter DH, Dobyns WB (2001) *LIS1* missense mutations cause milder lissencephaly phenotypes including a child with normal IQ. Neurology 57: 416–422

Liscovitch, M, Cantley LC (1995) Signal transduction and membrane traffic: the PITP/phosphoinositide connection. Cell 81:659–662

Lo Nigro C, Chong CS, Smith AC, Dobyns WB, Carrozzo R, Ledbetter DH (1997) Point mutations and an intragenic deletion in *LIS1*, the lissencephaly causative gene in isolated lissencephaly sequence and Miller-Dieker syndrome. Hum Mol Genet 6:157–164

Martin CL, Waggoner DJ, Wong A, Uhrig S, Roseberry JA, Hedrick JF, Pack SD, Russell K, Zackai E, Dobyns WB, Ledbetter DH (2002) "Molecular rulers" for calibrating phenotypic effects of telomere imbalance. J Med Genet 39: 734–740

McHale JC, McKie AB, Tarttelin EE, Inglehearn CF (2000) Expression map of human chromosome region 17p13.3, spanning the RP13 dominant retinitis pigmentosa locus, the Miller-Dieker lissencephaly syndrome (MDLS) region, and a putative tumour suppressor locus. Cytogenet Cell Genet 88:225–229

Morrow B, Goldberg R, Carlson C, Das Gupta R, Sirotkin H, Collins J, Dunham I, O'Donnell H, Scambler P, Shprintzen R, Kucherlapati R (1995) Molecular definition of the 22q11 deletions in velo-cardio-facial syndrome. Am J Hum Genet 56:1391–1403

Mutchinick OM, Shaffer LG, Kashork CD, Cervantes EI (1999) Miller-Dieker syndrome and trisomy 5p in a child carrying a derivative chromosome with a microdeletion in 17p13.3 telomeric to the LIS1 and the D17S379 loci. Am J Med Genet 85:99–104

Osborne LR, Herbrick JA, Greavette T, Heng HH, Tsui LC, Scherer S (1997) PMS2-related genes flank the rearrangement breakpoints associated with Williams syndrome and other diseases on human chromosome 7. Genomics 45: 402–406

Pilz DT, Matsumoto N, Minnerath SR, Mills P, Gleeson JG, Allen KM, Walsh CA, Barkovich AJ, Dobyns WB, Ledbetter DH, Ross ME (1998*a*) LIS1 and XLIS (DCX) mutations cause most classical lissencephaly, but different patterns of malformation. Hum Mol Genet 7:2029–2037

Pilz DT Macha ME, Precht KS, Smith AC, Dobyns WB, Ledbetter DH (1998*b*) Fluorescence in situ hybridization analysis with *LIS1* specific probes reveals a high deletion mutation rate in isolated lissencephaly sequence. Genet Med 1: 29–33

Plummer SJ, Simmons JA, Adams L, Casey G (1997) Mapping of 228 ESTs and 26 genes into an integrated physical and genetic map of human chromosome 17. Genomics 45: 140–146

Reichman CT, Mayer BJ, Keshav S, Hanafusa H (1992) The product of the cellular crk gene consists primarily of SH2 and SH3 regions. Cell Growth Differ 3:451–460

Sasaki S, Shionoya A, Ishida M, Gambello MJ, Yingling J, Wynshaw-Boris A, Hirotsune S (2000) A LIS1/NUDEL/Cytoplasmic Dynein Heavy Chain complex in the developing and adult nervous system. Neuron 28:681–696

Stack M, Jones D, White G, Liscia DS, Venesio T, Casey G, Crichton D, Varley J, Mitchell E, Heighway J (1995) Detailed mapping and loss of heterozygosity analysis suggests a suppressor locus involved in sporadic breast cancer within a distal region of chromosome band 17p13.3. Hum Mol Genet 4:2047–2055

Tsuda M, Tanaka S, Sawa H, Hanafusa H, Nagashima K (2002) Signaling adaptor protein v-Crk activates rho and regulates cell motility in 3Y1 rat fibroblast cell line. Cell Growth Differ 13:131–139

Van Tuinen P, Rich DC, Summers KM, Ledbetter DH (1987) Regional mapping panel for human chromosome 17: application to neurofibromatosis type 1. Genomics 1:374–381

Yaffe MB (2002) How do 14-3-3 proteins work?—Gatekeeper phosphorylation and the molecular anvil hypothesis. FEBS Letter Review 513:53–57